EXPONENTIAL-BASED SPIRAL DYNAMIC ALGORITHM FOR MODELLING OF A FLEXIBLE MANIPULATOR SYSTEM

Nasir, A. N. K.[1], Ismail, R. M. T. R. [1], Ahmad M. A.[1] and Tokhi. M. O.[2]
[1]Faculty of Electrical and Electronics Engineering, Universiti Malaysia Pahang, Pekan, Malaysia
[2]Department of Automatic Control and Systems Engineering, University of Sheffield, United Kingdom
E-Mail: kasruddin@ump.edu.my

ABSTRACT

This paper presents an exponential-based spiral dynamic algorithm (SDA) as an improved version of the original SDA. A simple structure with a unique feature of a spiral model in SDA leads the algorithm achieving fast convergence speed and short computation time. However, adopting a constant radius and a constant angle into the spiral model of SDA causes the algorithm to trap into local optima solution. To overcome the problem, both radius and angle of the spiral model is adaptively varied throughout the search process. It can be done by incorporating an exponential-based radius and an exponential-based angle into the spiral model of SDA. The algorithm is applied to solve dynamic modeling problem of a single-link flexible manipulator system. Results of the dynamic model show the proposed algorithm and the original SDA estimate adequate model and capture good dynamic behaviour of the system. However, the proposed algorithm acquires better model for the system compared to its predecessor algorithm.

Keywords: Spiral dynamic algorithm; system identification; flexible manipulator system.

INTRODCUTION

Flexible manipulator system (FMS) is used in the manufacturing industry as a tool in the production process. In general, FMS is a single-input multi-output system comprising rigid and flexible dynamics. An electromechanical actuator at the hub of the system produces rotational motion of a rigid body while a flexible beam joining the rigid body and a payload produces vibrational motion at the end point of the system. The natural vibrational behaviour of the system poses control challenges in applications where positional accuracy is required. However, the flexible structure of the system exhibits a lot of benefits over its rigid counterpart. Unlike a rigid manipulator, it is lighter in weight, has a smaller actuator, better mobility, consumes less power, is less expensive, operates cost-efficiently, has higher payload to robot weight ratio and offers more safety to the user [1], [2]. The research on FMS is increasingly gaining attention from researchers worldwide. The application of such system can be extensively found in various sectors such as in robotics [3], avionics [4]. This is due to the numerous advantages they offer compared to their rigid counterparts.

Modeling of a flexible manipulator system is a challenging task. Its vibrational behaviour and nonlinear characteristics make the modelling of such system a challenge and lead to complex mathematical model. However, this is an important area to study because it provides essential information about physical behavior of a system or a process. In fact, the information contained in the acquired model can be used to make further analysis on the system stability, system characteristics under different operating conditions, or as a principal knowledge for designing a control system. One of well-known approaches to acquire a mathematical model of the flexible manipulator system is a system identification approach.

System identification usually refers to acquiring the mathematical model of a dynamic system based on input-output experimental data captured from a real system [5]. System identification is extensively used in various applications. The advantage of system identification compared to conventional modelling approach is that a system can be modeled accurately without prior knowledge or physical information of the system. The existence of optimization algorithms and powerful computing technology make this method easy to implement, reliable and more importantly offer high accurate model. A well-known system identification approach used by researchers to acquire a dynamic model for flexible manipulator system is a parametric identification technique.

Over the years, parametric modeling approach has been widely used in dynamic modeling of the FMS. Many researchers have utilized metaheuristic algorithms and other well-known estimation methods to identify the unknown parameters in a parametric model structure, which has been found to be more simple and accurate. Besides, with the increasing efficiency in the computational tools nowadays, optimization algorithms are viewed as the efficient tools. For example, in dynamic modeling of an FMS, [6] adopted particle swarm optimization (PSO) to optimize autoregressive moving average (ARMA) model. [7] adopted genetic algorithm (GA) to optimize autoregressive moving average with exogenous input (ARMAX) model. On the other hand, [8] used bacterial foraging algorithm (BFA) to optimize ARX model. [9] adopted Nelder-Mead (NM) simplex method to optimize the parameters of a transfer matrix model. Dynamic modeling of the FMS based on spiral dynamic algorithm (SDA) is presented in [11], [12].

This paper presents an application of exponential-based Spiral dynamic algorithm (Eb-SDA) to dynamic modeling of the FMS. The Eb-SDA improves the accuracy performance of the original SDA introduced in [10]. It is proposed as an alternative strategy to SDA, which has a premature convergence due to incorporation of a constant radius and a constant angle into its spiral model. This paper is organized as follows. Section 1 presents the introduction of the paper. Section 2 describes the specification of flexible manipulator system. Dynamic modelling strategy of the FMS is explained in Section 3. Detail explanation of the proposed Eb-SDA is presented in Section 4 while the implementation and its corresponding result for dynamic modelling of the FMS is presented in Section 5. The paper is concluded in Section 6.

FLEXIBLE MANIPULATOR SYSTEM

A schematic diagram of the single-link FMS rig is shown in Figure-1 [13]. The system consists of a single flexible link made of aluminum beam and attached to an electromechanical motor. A U9M4AT type printed circuit board with bi-directional drive amplifier is used to rotate the motor shaft in both counterclockwise and clockwise directions. As there are three outputs of interest to be gauged from the system, three different sensor units are incorporated into the system. An integrated circuit piezoelectric accelerometer is placed at the tip of the beam and used to measure end-point acceleration. The advantages of the sensor are that it is small in size, light in weight, has high voltage sensitivity and low impedance output, which prevent significant amount of signal losses and distortion problems. An encoder with a resolution of 2,048 pulses/revolution and a tachometer are attached to the motor shaft and used to measure hub-angle and hub-velocity respectively. Moreover, a personal computer (PC) embedded with Pentium Celeron 500 MHz processor is connected with PCL818G interfacing unit to the FMS. Matlab/ Simulink software installed in the PC is used as a tool for controlling and manipulation of the system.

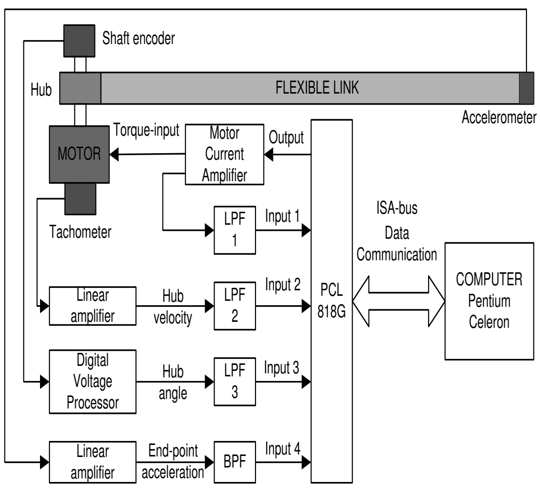

Figure-1. Condition when wheel zigzag gets over block.

MODELLING OF FLEXIBLE MANIPULATOR SYSTEM

Modeling phase

The parametric modelling strategy with metaheuristic algorithm employed for both systems is depicted in Figure-2. Autoregressive with exogenous (ARX) model is selected for the parametric model structure. The general expression of the ARX is represented as:

$$\frac{Y(z)}{U(z)} = \frac{\sum_{j=0}^{M} b_j z^{j}}{1+\sum_{i=1}^{N} a_i z^{i}} \quad (1)$$

where N is the order of the transfer function and the number of poles present in the system. M is the order of numerator and the number of zeros presents in the system. An accurate and stable dynamic model of a system can be developed by determining the unknown coefficients of the denominator and numerator through an optimization technique. The $\hat{y}(t)$ is the predicted output while $y(t)$ and $u(t)$ are recorded output-input from the experimental system. The $e(t)$ is the modelling error and is used in formulating the cost function for the optimisation algorithm.

In this work, RMSE with gain function is selected as a minimisation cost function with the optimization algorithms. In dealing with constraint in the modelling phase, a penalty function can be incorporated into the cost function. For a stable discrete transfer function of a dynamic system, all poles must lie within the unit circle (in the z-plane). If there is any pole of the discrete transfer function outside the unit circle, then the solution must be disregard even if the magnitude of the error function is very small.

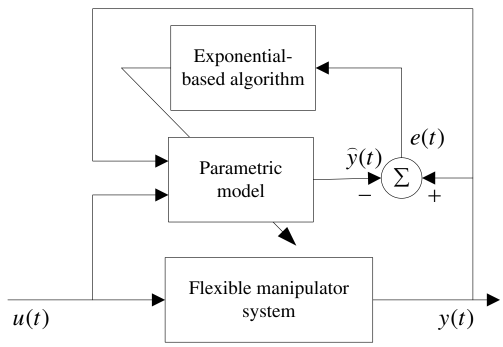

Figure-2. Block diagram for parametric modeling with metaheuristic algorithm.

The solution is penalised by adding a large constant value to the error function. The cost function with penalty approach is thus defined as:

ARPN Journal of Engineering and Applied Sciences

www.arpnjournals.com

$$f(t) = \left(\frac{1}{K} \sqrt{\sum_{t=1}^{K} e^2(t)} \right) w \qquad if\, all\, poles\ in |z| < 1 \quad (2)$$

$$f(t) = \frac{1}{K} \sqrt{\sum_{t=1}^{K} e^2(t)} \div w + penalty gain \qquad else \quad (3)$$

where K is total number of sampled data, e is the difference between actual and predicted outputs as shown in Figure-2 and w is a gain factor. Since the error is squared, this cost function has more chances to reduce large errors. The gain factor is used to amplify the function value in case extremely small error is produced. The penalty gain in Equation. (3) can be defined as a large constant value. Incorporating such approach into the optimization algorithm may give a stable solution for the whole iterations.

Validation phase

In this work, two types of tests are conducted to evaluate the adequacy of a predicted model to represent the actual system. If only the estimated model passes all the tests, then it can be considered as adequate and acceptable to represent the actual system. However, if it does not pass at least one of the tests, then the modelling process must be repeated.

Experimental input-output data. The actual input-output data recorded during experimental exercise can be separated into modelling and validation parts. In practice, the first two-thirds of the data is used to estimate the model in the modelling phase while the remaining data can be used to check the predicted model validity in the validation phase [5]. Ideally, the output of the predicted model must portray exactly the same signal as the second portion of the actual output if the actual input is applied to the estimated model. A block diagram for linear parametric system identification used to validate the estimated model of a system is depicted as in Figure-3.

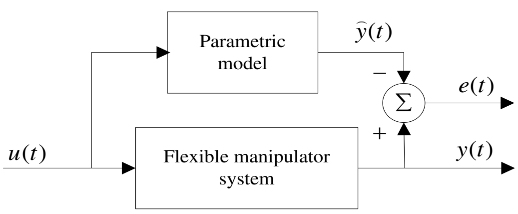

Figure-3. Block diagram to validate the estimated model.

Stability test. The stability test is normally conducted through determination of poles of a discrete or a continuous transfer function. A discrete model is considered as stable if all poles lie within the unit circle in the z-plane. On the other hand, a continuous model is regarded as stable if all poles lie in the left hand side of S-plane.

EXPONENTIAL-BASED SPIRAL DYNAMIC ALGORITHM

In adaptive SDA, instead of constantly changing the step size through constant spiral radius and rotational angle or angular displacement, the step size is varied dynamically based on fitness cost value of current search point location in the search space. This is realized by varying the spiral radius, r and angular displacement, in the spiral equation. This novel approach contributes to better accuracy since the movement of the search point is guided by fitness cost value of points in the search space.

In exponential-based SDA, the fitness deviation $|f(x_i(k)) \;\; \min J|$ is formulated in an exponential form. Through exponential formulation of fitness deviation value, the spiral radius and the step size of a search point are changed dynamically in exponential manner. Compared to linear approach, exponential formulation helps the search point to further accelerate towards best location. The mathematical formulation of Eb-SDA is given as:

$$r_{eb} = \frac{(r_l - r_u)}{\left(1 + \left(\frac{c_1}{\exp\left(c_2\left(|f(x_i(k)) - \min J|\right)\right)}\right)\right)} + r_u \quad (4)$$

where r_{eb} is exponential-based spiral radius, c_1 and c_2 are tuneable constants, determined heuristically. In case of small $|f(x_i(k)) \;\; \min J|$, the exponential function causes the term $c_1 / \exp\left(c_2\left(|f(x_i(k)) \;\; \min J|\right)\right)$ to have extremely large value. As a result, r_{eb} is big or approaching maximum spiral radius, r_u. On the other hand, positive constant value of c_1 is rate of change of fitness value and spiral radius. Small value of c_1 tends to select maximum radius, r_u while big value of c_1 tends to select minimum radius, r_l. The tuneable scaling constant c_2 is used to scale $|f(x_i(k)) \;\; \min J|$ so that r_{eb} is not too big when $|f(x_i(k)) \;\; \min J|$ is big or r_{eb} is not too small when $|f(x_i(k)) \;\; \min J|$ is small. In case of similar value of $|f(x_i(k)) \;\; \min J|$, the exponential term of fitness deviation in Equation. (4) produces a steep slope of spiral radius versus fitness deviation value. This indicates that the search point has higher acceleration towards global best location.

For the Equation. (4) to be working properly, $|f(x_i(k)) \;\; \min J|$ must not be equal to zero. Therefore, a mechanism must be defined to avoid the failure of the algorithm to complete the search operation. In this work, if condition $|f(x_i(k)) \;\; \min J| = 0$ is met, a random r_{eb} between $[r_l, r_u]$ for the respective search point is generated. This mechanism enables the search point to move away from its original location before continuing the search operation.

ARPN Journal of Engineering and Applied Sciences

Table-1. Parameters of exponential-based SDA.

Symbol	Description
$\theta_{i,j}$	Search point angular displacement or rotational angle on $x_i - x_j$ plane around the origin.
r	Spiral radius to be replaced by adaptive approach as in step 2 of Figure-4.
m	Total number of search points.
k_{max}	Maximum iteration number.
$x_i(k)$	Position of i_{th} point in k_{th} generation.
R^n	Composition of rotational $n \times n$ matrix based on combination of all 2 axes.

Set initial points $x_i(0) \in R^n, i = 1,2,...m$ in the feasible region at random and centre x^* as $x^* = x_{i_g}(0)$, $i_g = \arg\min_i f(x_i(0)), i = 1,2,...,m$.

Step 2: Updating x_i

$x_i(k+1) = S_n(r,\theta)x_i(k) - (S_n(r,\theta) - I_n)x^*$,
$i = 1,2,...,m$
where spiral radius, r replaced by r_{eb}, or angular displacement, θ replaced by θ_{eb} as shown in Eqn. (4).

Step 3: Updating x^*

$x^* = x_{i_g}(k+1)$,
$i_g = \arg\min_i f(x_i(k+1)), i = 1,2,...,m$

Step 4: Checking termination criterion

If $k = k_{max}$ then terminate. Otherwise set $k = k+1$, and return to step 2.

Figure-4. Step-by-step description of exponential-based spiral dynamic algorithm.

IMPLEMENTATION AND RESULT

Naturally, vibration will occur when an external force is applied on a flexible structure. In the FMS case, vibration occurs due to fast motion. This is measured by an accelerometer placed at the end point of the flexible beam. FMS response consists of three resonance modes within 0-100 Hz. Thus, to model the end-point acceleration behaviour over 0-100 Hz, at least three pairs of complex conjugate poles are required resulting in a sixth-order transfer function. However, incorporating the rigid body dynamics of the FMS, an eight-order ARX model is considered for end-point acceleration [8].

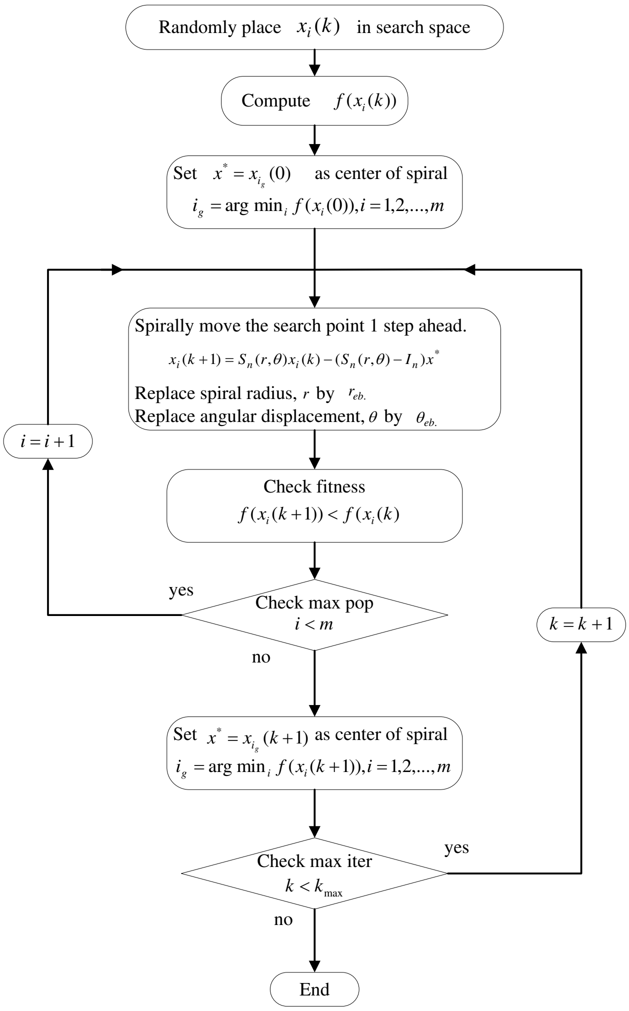

Figure-5. Flow chart of exponential-based spiral dynamic algorithm.

Substituting $N = 8$ and $M = 7$ in Equation. (5), the ARX structure for the dynamics model can be defined as:

$$\frac{Y(z)}{U(z)} = \frac{\sum_{j=0}^{7} b_j z^{1}}{1 + \sum_{i=1}^{8} a_i z^{1}} \tag{5}$$

The ARX model for the system can be represented in discrete transfer function form as:

$$\frac{Y(z)}{U(z)} = \frac{b_0 z^8 + b_1 z^7 + b_2 z^6 + b_3 z^5 + b_4 z^4 + b_5 z^3 + b_6 z^2 + b_7 z}{z^8 + a_1 z^7 + a_2 z^6 + a_3 z^5 + a_4 z^4 + a_5 z^3 + a_6 z^2 + a_7 z^1 + a_8} \tag{6}$$

Equation. (6) has resulted in 16 coefficients of numerator, b_0-b_7 and denominator, a_1-a_8 in which the value is unknown. All the coefficients defined previously will be estimated and optimized by the proposed

VOL. 10, NO. 23, DECEMBER 2015 ISSN 1819-6608
ARPN Journal of Engineering and Applied Sciences

optimization algorithm. User-defined parameters for the proposed algorithm to optimize end-point acceleration model were heuristically defined through trial and error based approach. They are shown in Equations. (7) and (8).

$$r_{eb} = \frac{(0.1-1)}{\left(1+\left(\frac{100}{\exp(1.5(|\,f(x_i(k))-\min J\,|))}\right)\right)}+1 \qquad (7)$$

$$_{eb} = \frac{(0.1 \quad 2\ )}{1+\frac{10}{\exp((|\,f(x_i(k)) \quad \min J|))}}+2 \qquad (8)$$

Numerical results of the modelling and validation parts are shown in Table-2 while graphical results for the modelling and validation parts are presented in time-domain and frequency-domain as shown in Figures 6 and 7. For Table-2, the best result is highlighted in bold font. It is noted that the proposed algorithm achieved better accuracy at 17.83 than the original SDA, which has accuracy at 35.83. It also shown that the proposed algorithm resulted in smaller error range in both modelling and validation phase.

Table-2. Performance of SDA and exponential based SDA.

Algorithm	Best fitness, f_x	Range of error	
		Modelling	Validation
SDA	35.85	[-0.1159, 0.1074]	[-0.1355, 0.1458]
Exponential-based SDA	**17.83**	**[-0.0614, 0.0638]**	**[-0.0642, 0.0629]**

Convergence plot of the optimization algorithms is shown in Figure-6a. It shows that the original SDA leads the convergence graph at the early iteration. However, at the time reached 73 seconds, exponential-based SDA graph successfully intercepted original SDA graph. It converged further towards the end of the iteration to give a fitness value 17.83. SDA trapped at local optima solution with fitness value 35.85 starting at 1460 seconds and it unable to converge further until the end of the search operation. Figure-6b shows that end-point acceleration response of FMS acquired by both algorithms almost coincide with the actual signal recorded from real hardware. However, the response optimized by the proposed algorithm achieved smaller error as shown in Figure-6c.

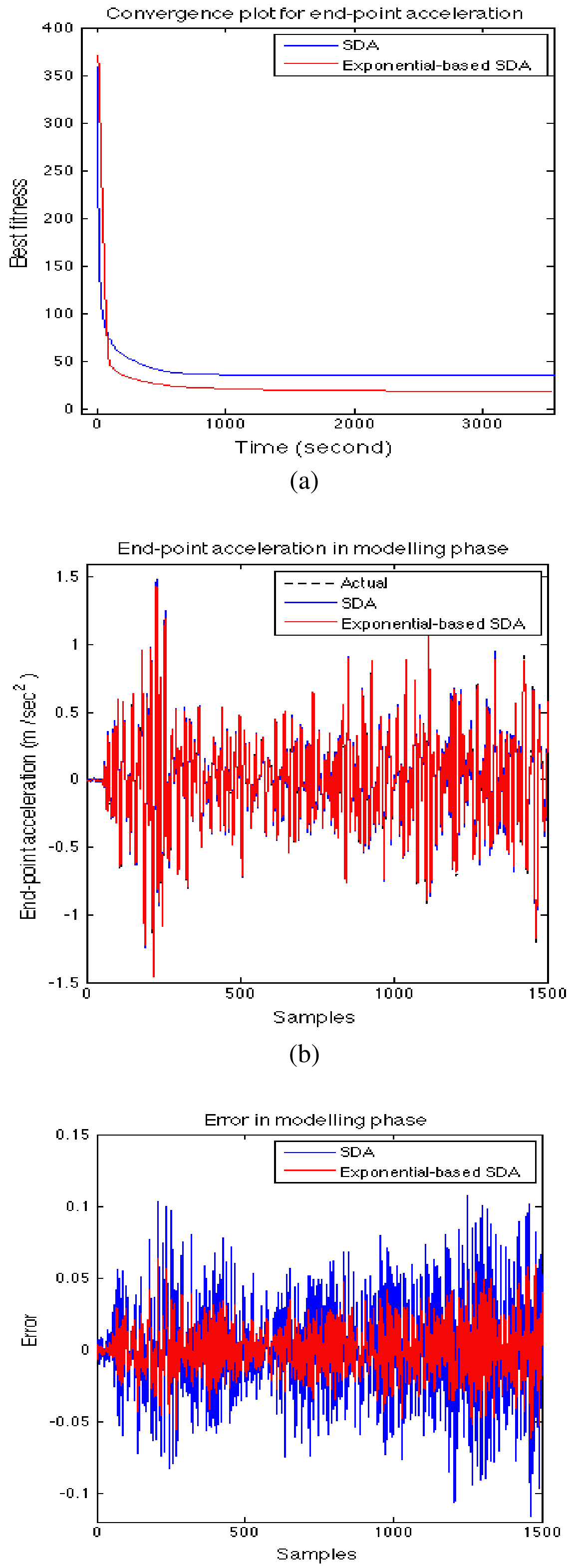

(a)

(b)

(c)

Figure-6. Result in modeling phase. a) Convergence plot, b) Time-domain response and c) error.

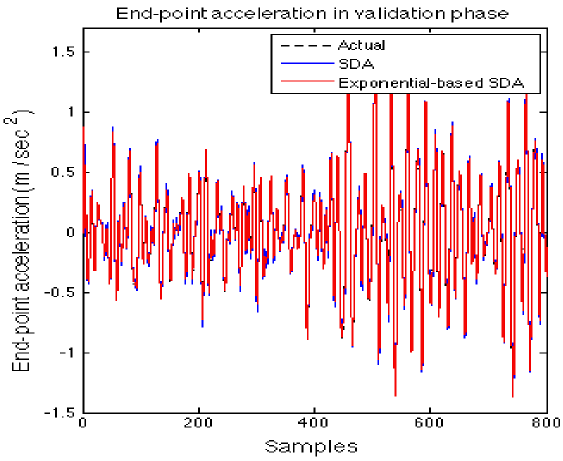

(a)

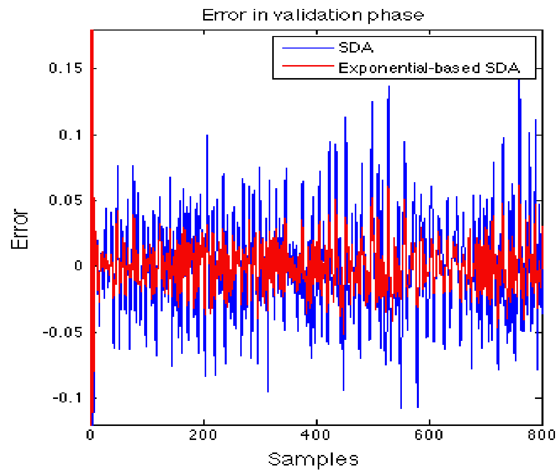

(b)

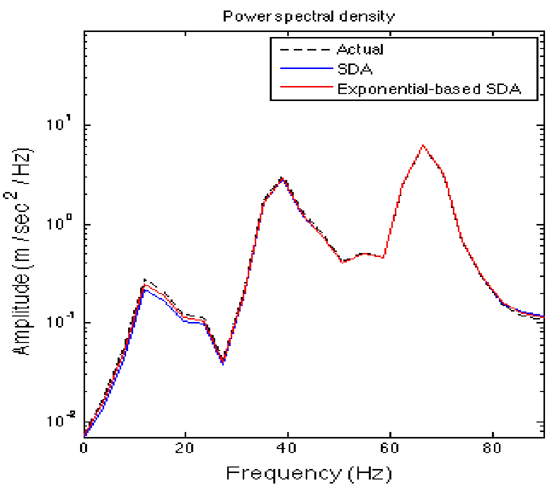

(c)

Figure-7. Result in validation phase. a) Time-domain response, b) error and c) Frequency-domain plot.

Time-domain response of the end-point acceleration in validation phase is shown in Figure-7a. It shows that the response attained by both algorithms almost follow the actual signal. However, the proposed algorithm acquired better response since it has smaller error as shown in Figure-7b. Frequency-domain plot in Figure-7c shows that the estimated models from both algorithms successfully captured a dynamic behaviour of the end-point acceleration. In practice, end-point acceleration should consist three modes of resonance frequencies. From the figure, they are found at 11.72 *Hz*, 39.06 *Hz* and 66.41 *Hz*. The first mode of the resonance frequency shows that the exponential-based SDA graph is more identical to the actual signal than the SDA graph.

Transfer function of the estimated end-point acceleration optimized by both SDA and exponential-based SDA is shown in Eqnuations. (9) and (10) respectively. Stability test was conducted on both transfer functions based on poles and zeros location in a unit-circle. From the test, all the poles are found inside the unit-circle, which indicates that the transfer functions are stable. Moreover, those two transfer functions are found as observable and controllable. This was tested using observability and controllability tools in Matlab software.

$$H(z)_{SDA} = \frac{0.01916Z^7 \;\; 0.01191Z^6 \;\; 0.005592Z^5 \;\; 0.01978Z^4 + 0.003867Z^3 + 0.01559Z^2 + 0.006081Z + 0.01818}{Z^8 \;\; 1.617Z^7 \;\; 0.3437Z^6 + 1.848Z^5 \;\; 0.198Z^4 \;\; 0.9938Z^3 + 0.103Z^2 + 0.413Z \;\; 0.102} \quad (9)$$

$$H(z)_{eb} = \frac{0.00101Z^7 \;\; 0.00059Z^6 + 0.00344Z^5 \;\; 0.000385Z^4 + 0.000261Z^3 + 0.000846Z^2 + 0.00694Z + 0.00556}{Z^8 \;\; 2.492Z^7 + 1.805Z^6 + 0.5301Z^5 \;\; 1.094Z^4 + 0.145Z^3 + 0.0393Z^2 + 0.268Z \;\; 0.1533} \quad (10)$$

CONCLUSIONS

An exponential-based spiral dynamic algorithm (SDA) which is the improved version of original SDA has been proposed. A mathematical exponential function has been adopted to vary radius and angle of a spiral model in SDA throughout the searh operation. It improves the accuracy while retaining a simple structure of the original SDA.

The proposed algorithm has been applied to attain a dynamic model of a flexible manipulator system in comparison to original SDA. A parametric modelling approach with ARX structure has been adopted in the design. Results of the work have been presented in time domain and frequency domain. It can be concluded that that both algorithms successfully acquire adequate and good dynamic models. However, the proposed algorithm has estimated better model and contain less error compared the original SDA.

In the future, the proposed algorithm will be extended to multiobjective algorithm. In terms of the application, the proposed algorithm will be applied to model the flexible manipulator system through nonparametric modelling approach.

REFERENCES

[1] Ostergaard E. H. 2012. Lightweight robot for everybody. IEEE Robotics & Automation Magazine, Vol. 19, No. 4, pp. 17–18.

[2] Tokhi M. O., Mohamed Z., Amin S. H. M. and Mamat R. 2000. Dynamic characterization of a flexible manipulator system: theory and experiments, Proceedings of TENCON 3, Kuala Lumpur, 24-27 September 2003, pp. 167–172.

[3] Gharooni S., Heller B., Tokhi M. O. 2001. A new hybrid spring orthosis for controlling hip and flexion in the swing phase. IEEE Transaction Neural System Rehabilitation Engineering, Vol. 9, No. 1, pp. 106 - 107.

[4] Hu Q. 2009. Variable structure maneuvering control with time-varying sliding surface and active vibration damping of flexible spacecraft with input saturation, Acta Astronautica, Vol. 64, No. 11–12, pp. 1085 - 1108.

[5] Ljung L. 1999. System identification: theory for the user 2nd edition. Englewood Cliffs, HJ: Prentice hall.

[6] Alam M. S. and Tokhi M. O. 2007. Dynamic modeling of a single-link flexible manipulator system: a particle swarm optimization approach. Journal of Low Frequency Noise, Vibration and Active Control, Vol. 26, No. 1, pp. 57 – 72.

[7] Shaheed M. H. and Tokhi M. O. 2002. Dynamics modelling of a single-link flexible manipulator: parametric and non-parametric approaches. Robotica, Vol. 20, No. 1, pp. 93 – 109.

[8] Supriyono H. and Tokhi, M. O. 2012. Parametric modeling approach using bacterial foraging algorithms for modeling of flexible manipulator systems. Engineering Applications of Artificial Intelligence, Vol. 25, No. 5, pp. 898 – 916.

[9] Krauss R.W., 2011. Computationally efficient modeling of flexible robots using the transfer matrix method. Journal of Vibration and Control, Vol. 18, No. 5, pp. 596–608.

[10] TamuraK. and Yasuda K. 2011. Spiral multipoint search for global optimization. Proceeding of 10th International Conference on Machine Learning and Applications, pp. 470 – 475.

[11] Nasir A.N.K., Tokhi M.O., Ghani N.M.A., Ismail R.M.T.R. 2012. Novel adaptive spiral dynamic algorithms for global optimization. Proceeding of 2012 IEEE 11th International Conference on Cybernetic Intelligent Systems (CIS), 23-24 Aug. 2012, pp. 99-104.

[12] Nasir A.N.K., Tokhi M.O., Sayidmarie O., Ismail R.M.T.R. 2013. A novel adaptive spiral dynamic algorithm for global optimization. Proceeding of 2013 13th UK Workshop on Computational Intelligence (UKCI), Surrey, UK, 9-11 Sept. 2013, pp. 334-341.

[13] Azad A. K. M. 1994. Analysis and design of control mechanisms for flexible manipulator systems. PhD Thesis, Department of Automatic Control and Systems Engineering, The University of Sheffield, UK.